RSC Advances

ROYAL SOCIETY OF CHEMISTRY

www.rsc.org/advances

The large electrochemical capacitance of nitrogen-doped mesoporous carbon derived from egg white by using a ZnO template

Jiucun Chen,*[abc] Yinqin Liu,[abc] Wenjun Li,[abc]

Huan Yang[abc] and Liqun Xu [abc]

[a]*Institute for Clean Energy & Advanced Materials, Southwest University, Chongqing 400715, P.R. China. E-mail: chenjc@swu.edu.cn; Fax: +86-023-68254969; Tel: +86-023-68254795*

[b]*Chongqing Key Laboratory for Advanced Materials & Technologies of Clean Energies, Chongqing 400715, P.R. China*

[c]*Faculty of Materials and Energy, Southwest University, Chongqing 400715, P.R. China*

In this paper, a novel hierarchically structured mesoporous carbon material doped with nitrogen is prepared by using a two-step template method, of which egg white is the precursors of carbon and the nanostructured ZnO is the template. The unique composition and structure of the carbons resulted in very promising electrochemical energy storage performance. Tested as a supercapacitor, the carbons exhibited a capacitance of 205 F g^{-1} at discharge current density of 0.5 A g^{-1}; and, its cyclic performance is dramatically enhanced sustaining greater than 97% of its original capacitance after 5000 charge-discharge cycles. This work displays a simple method to preparing porous carbon electrodes, and provides a vivid example to rationally produce carbon materials from natural sources in pseudocapacitor.

1. Introduction

Supercapacitors play an important role in energy conversion and storage system due to their higher power density, longer life cycle in comparison to batteries/fuel cells and higher energy density over traditional dielectric capacitors.[1,2] According to the different mechanism of charge storage, supercapacitors can be categorized into two major classes, electrochemical double-layer capacitor (EDLC) and pseudocapacitor, which store charge using non-faradic charge accumulation at interfacial double layer of electrode and electrolyte for EDLC and fast surface redox reactions for pseudocapacitors.[3-6] The EDLC has been recognized as an efficient energy storage device because of its higher power density and longer cycle life as compared to the pseudocapacitors.[7,8] Carbon materials including activated porous carbons are used widely in the electrode materials of EDLC due to their good electrical conductivity, chemical stability and high surface area.[9-11] In aqueous electrolytes, the vast majority of EDLCs are based on high surface area microporous activated carbons and related materials.[12] Carbon materials with highest capacitances in aqueous electrolytes are those with both high surface areas and high surface heteroatom contents (such as O, N and B), derived from precursors rich in those elements.[13-16] The N-doped carbons also possess improved electrical conductivity compared to their pure counterparts.[17] In our daily life, there are large quantities of protein-rich biomasses available, such as dates' stones, coconut shells, pitch coke, wood, rice husk, walnut shell, banana peel and fungi,[18-27] most of which are focus on the abundant porous structure to improving the surface area.[28] Millions of industrial-grade chicken eggs with special additives are employed to cultivate various antibodies from the egg yolk or to extract "all natural" chemicals for anti-microbial and cosmetic industries.[29] This process generates large quantities of nonedible chicken egg-based waste, waiting for value-added green energy applications. In fact, proteins, as a biopolymer containing the highest nitrogen concentration in bio-organism, play a key role in electron transfer and energy conversion processes in biological systems.[30] The physical and chemical properties of eggs have been thoroughly studied by food chemists. Egg white contains

around 90% water and 10% proteins, including ovalbumin, ovotransferrin, ovomucoid and small amounts of other proteins. Unlike plant-based precursors, these proteins are naturally rich in nitrogen, containing on average 15% N by weight.[31]

Numerous novel methods for designing the porous structure of carbon materials have been lately developed. Among them, template carbonization is a distinct and versatile approach for supplying well-designed and nearly totally pore controlled carbon materials.[32,33] However, low carbon yield, and process issues, which are the consequence of a time consuming wet silica etching process (template removal) as well as further purification steps lead to economic and ecologic drawbacks. Thus, there is still need to find better template and seek optimal synthesis conditions to produce activated carbon electrode material.

The use of zinc oxide (ZnO) as templating materials possesses several unique merits. For instance, ZnO can be easily produced in a wide variety of morphologies including nanoparticles, nanorods, tubes, disks and other complex nanostructures.[34,35] In addition, ZnO being amphoteric in nature, can be easily dissolved in mild acids or bases and hence removal would be simple.[36] In this study, we used inexpensive and commercially available ZnO nanoparticles as hard template and egg white as precursors to successfully synthesize the nitrogen-doped mesoporous carbon materials. The carbon electrodes showed a specific capacitance of 205 F g^{-1} at discharge current density of 0.5 A g^{-1} and maintained 97% of the initial specific capacitance after 5000 charge-discharge cycles with good electrochemical stability.

2. Experimental section

2.1 Materials

The eggs were obtained from supermarket. Nanoparticle ZnO (diameter: 30~40 nm) were purchased from Xiya Reagent Research Center. Deionized (DI) water was used throughout the experiments.

2.2 Synthesis of doped porous carbon materials

The mesoporous carbon samples are prepared by utilizing different carbonization conditions. Briefly, in a typical synthesis, a mixture of egg whites (0.8 g) and ZnO

template (0.4 g) was grounded using a mortor for 5 min. Then the mixture was transferred into a crucible and the carbonization was completed by a pyrolysis at 800 ^{o}C (5 ^{o}C min^{-1}) for 2 h under argon atmosphere. The as-prepared composites obtained after the pyrolysis were washed with excess 1 M HCl and DI water to remove the ZnO templates, and dried at 60 °C overnight in a vacuum. According to the different mass ratios of egg white to ZnO, the as-prepared products were named as C-1 ($m_{egg\ white}$: m_{ZnO} = 1:1), C-2 ($m_{egg\ white}$: m_{ZnO} = 2:1), C-3 ($m_{egg\ white}$: m_{ZnO} = 3:1) and C-4 ($m_{egg\ white}$: m_{ZnO} = 4:1) (denoted as C-X, X is corresponding to the 1, 2, 3 and 4). For comparision, the template-free bare egg white carbon was produced by using the same conditions in the absence of ZnO，further denoted as FC. The mixture of egg whites (0.8 g) and ZnO template (0.4 g) was treated in later by using the same conditions at different carbonization temperature (from 600 ^{o}C to 900 ^{o}C) and labelled as C-2-Y, Y is corresponding to the 600, 700, 800 and 900 ^{o}C.

2.3 Material characterizations

The morphology and microstructure were examined by field-emission scanning electron microscopy (FESEM, JSM-6700F) and transmission electron microscopy (TEM, JEM-2100). X-ray photoelectron spectroscopy (XPS) was performed using 200 W monochromated Al Kα radiation (Thermo Scientic ESCALab 250Xi). The binding energies were calibrated based on the graphite C1s peak at 284.8 eV. Raman spectra were measured at room temperature by a Renishaw InVia Raman spectrophotometer with argon ion laser (λ = 514.5 nm) as the excitation light.

2.4 Electrochemical measurements

Except specific description, all the electrochemical characterizations were carried out in 1 M H_2SO_4 with a three-electrode cell using as prepared carbon, platinum foil and saturated calomel electrode (SCE) as work, counter and reference electrodes, respectively. As for the work electrode, a glassy carbon electrode (diameter of 4 mm^2) coated with paste of the as prepared active carbon and Nafion was used. Charge-discharge (CD) and cyclic voltammetry (CV) techniques were performed over -0.3 V to 0.8 V. All other electrochemical measurements were conducted with a CHI 660 electrochemical

workstation (Shanghai Chenhua Co., China). The specific capacitance is calculated as follows:

$$C = \frac{I^{*}\Delta t}{V^{*}m} \quad \text{(CD method)} \quad (1)$$

$$C = \frac{1}{2mVv}\int_{V-}^{V+} I(V)\,dV \quad \text{(CV method)} \quad (2)$$

Where C (F/g) is the specific capacitance, I (A) is the discharge current, Δt (s) is the discharge time, V (V) is the potential window, m (g) is the weight of the active material and v (V/s) is scan rate.

3. Results and discussion

3.1 Materials characterizations

Fig. 1 shows the FE-SEM images of the surface morphologies of various produced porous carbon materials. Fig. 1a-g clearly show that C-Xs and C-2-Ys have macro/meso-pore morphology formed by self-assembly of carbon sheets, which promote the electrolyte ions diffusion into the inner micro-pores at higher charging rates. However, there is no apparent surface morphology difference of C-Xs and C-2-Ys in the FE-SEM images. To clearly observing the microstructure of well-defined carbon appeared in C-2 (C-2-800), TEM and HRTEM were used to characterize C-2 (C-2-800). As shown in Fig. 2, the TEM image of C-2 further confirms that the carbon sheet obtains large amount of mesopores. The degree of ordering in a carbon is estimated by the intensity ratio between the G band (1600 cm^{-1}) and the D band (1350 cm^{-1}) of the Raman spectra (Fig. 3). The former corresponds to the graphitic order, while the latter corresponds to the degree of disordered/defectiveness in the structure. The N_2 adsorption-desorption isotherms curve shape of the as-prepared carbon in Fig. 4 show that the pores are formed by self-assembly of carbon nanosheets. According to Brunauer-Emmett-Teller (BET) analysis and the Barret-Joyner-Halenda (BJH) model, a total specific surface area and pore size of the produced carbon are obtained in Table 1, from which we can see that

the pore size of all carbons are mesopore of 9-20 nm, however, with the increase of egg white amount, the shell of carbon material becomes thicker and resulting smaller surface area for C-3 and C-4. The anneal temperature has great influence on the performance of carbon materials. Table 1 shows that the surface area of carbon becomes bigger when anneal temperature increase, however, it suddenly decrease when the temperature increased to 900 ^{o}C, the biggest surface area of synthesized carbon material goes to C-2-800, which indicate better capacitance property. Furthermore, the surface composition of C-2-800 is further tested by XPS in Fig.5, in which peaks of O1s, C1s, N1s are found conforming the presence of C, N and O elements in the carbon. In details, 71.84% of carbon, 6.22% of nitrogen and 14.18% of oxygen are obtained from the calculation.

3.2 Electrochemical behavior of the template mesopore carbons

The cyclic voltammogram (CV) curves of template mesopore carbons produced from different mass ratio of egg white and ZnO are presented in Fig. 6a at a scan rate of 50 mV s^{-1} from -0.3 V to 0.8 V. Fig. 6a shows that these curves with rectangular shape indicate their typical double-layer capacitor behavior, and the specific capacitances of C-1, C-2, C-3 and C-4 are 78.78, 162.82, 84.85 and 66.6 F g^{-1} respectively, much higher than the value of the template-free egg white carbon (15.27 F g^{-1}). However, there are clear the indication of increased ohmic drop (iR drop) in the case of C-3 in Fig. 6(a). This may be because the reduction of egg white concentration affects the contact of carbon layers and the formation of pore structures. Meanwhile, excessive egg white would lead to the accumulation of carbon layers, resulting bulk structure and less pores. The capacitance behavior is consistent with the BET result. The specific capacitance calculated from discharge time in current densities from 0.5 A g^{-1} to 30 A g^{-1} is given in Fig. 6(b). The specific capacitance shows small decrease even in high discharge current density of 30 A g^{-1}, indicating a good rate capacitance property. Among all the samples, C-2 proves the best in specific capacitance at all scan rates. This is consistent with the BET result. Fig. 6(c) represents the CVs for different carbonization temperatures at a scan rate of 50 mV s^{-1}. The rectangular nature confirms charge storage mainly by electrical double layer formation at the

electrode-electrolyte interface, however, samples produced in different carbonization temperature show pretty huge difference in CV enclosed area, indicating a different specific capacitance. We can see that with the temperature increasing, the CV area becomes bigger, however when temperature reaches to 900 ^{o}C, the CV area decreases. This is mainly because that the sample annealed at low temperature (C-2-600, C-2-700) shows weak electron conductivity and small specific surface area and that sample produced at high temperature (C-2-900) shows limited specific surface area and high crystallinity. Fig. 6(d) summarizes the specific capacitances calculated from the charge-discharge measurements for different charging rates from 0. 5 A g^{-1} to 30 A g^{-1}. At 0.5 A g^{-1}, C-2-800 provides a highest specific capacitance of 205 F g^{-1}, which is 1.07 and 1.3 times higher than that of C-2-700 (191 F g^{-1}) and C-2-900 (158 F g^{-1}), respectively. The rate capability of C-2-800 and C-2-900 is better than C-2-700, which is benefit from the high crystallinity at high annealing temperature. However, the pore structure is damaged and the low specific surface area for C-2-900 leads to smaller specific capacitance at all discharge current densities.

Fig. 7(a) shows the CVs of C-2-800 in the 1 M H_2SO_4 aqueous electrolyte for different scan rates in the potential window -0.3~0.8 V. The rectangular nature of the CV illustrates the double layer formation at the electrode-electrolyte interface and no redox reaction is seen to be involved. A small distortion of the rectangular nature at higher scan rates can be observed on account of the lower mesopore density and the series resistance. The capacitive behavior of the C-2-800 electrode is further confirmed from well-defined sloped galvanostatic charge-discharge (CD) curves obtained at different current densities from 0.5 to 30 A g^{-1} (Fig. 7(b)). A highest specific capacitance of 205 F g^{-1} is achieved at 0. 5 A g^{-1} and 128 F g^{-1} at 30 A g^{-1}, showing a pretty good rate capacitance property of C-2-800.

Nyquist plots of samples produced at different mass ratios of egg white to ZnO and different carbonization temperatures are represented in Fig. 8. All capacitors also have an equivalent series resistance (ESR), which is caused by the resistance of the solution, as well as the internal resistance of the electrode. Fig. 8(a) shows the Nyquist plots with well-defined semicircles over the high-frequency region of C-1, C-2 and C-4

electrodes, followed by a straight sloped line in the low-frequency region. However, the Nyquist plots of the C-3 display a bad linearity and have no semicircle. This may be caused by the poor capacity and the bigger ion diffusion resistivity, which is also consistent with the results of CV and CD measurements. Fig. 8(b) presents the Nyquist plots of samples at different carbonization temperature, it shows that the slope of the impedance gradually approaches to a straight line along the imaginary axis (Z″) from C-2-700, C-2-900 to C-2-800, implying the rapid ion diffusion ability of C-2-800. Long-term cycling of C-2-800 shows no obvious fade in capacitance even after 5000 cycles (Fig. 9). Its excellent stability indicates that no major changes in physical or chemical structure occur during the cycling process.

4. Conclusions

We have successfully synthesized a highly mesoporous carbon using egg white as carbon source and nano-sized ZnO as a template for an ideal electrode material in a supercapacitor. The obtained optimal mesoporous carbon exhibit superior performance with a capacitance of 205 F g^{-1} at 0.5 A g^{-1} in a 3-electrode cell and an excellent cycle life (97% retention after 5000 cycles) because of the lower ion diffusion resistance, bigger specific surface area and good electron conductivity, which is importance property in supercapacitor. This work displays a simple method to preparing porous carbon electrodes, and provides a vivid example to rationally produce carbon materials from natural sources in pseudocapacitor.

Acknowledgments

This work is financially supported by Chongqing Key Laboratory for Advanced Materials and Technologies of Clean Energies. We greatly appreciate the Program for the Fundamental Research Funds for the Central Universities (SWU 113075 and XDJK2014B015), Chongqing Postgraduate Science and Technology Innovation Project (CYS2015045) and Science and Technology Program of Beibei (2015-06).

References:

1 Y. L. Shao, M. F. El-Kady, L. J. Wang, Q. H. Zhang, Y. G. Li, H. Z. Wang, M. F. Mousavi and R. B. Kaner, *Chem. Soc. Rev.*, 2015, **44**, 3639-3665.

2 C. Zhong, Y. D Deng, W. B. Hu, J. L. Qiao, L. Zhang and J. J. Zhang, *Chem. Soc. Rev.*, 2015, **DOI:** 10.1039/C5CS00303B.

3 K. Naoi, S. Ishimoto, J. Miyamoto and W. Naoi, *Energy Environ. Sci.*, 2012, **5**, 9363-9373.

4 A. S. Arico, P. Bruce, B. Scrosati, J. M. Tarascon and W. V. Schalkwijk, *Nat. Mater.* , 2005, **4**, 366-377.

5 P. Simon and Y. Gogotsi, *Nat. Mater.*, 2008, **7**, 845-854.

6 G. Wang, L. Zhang and J. Zhang, *Chem. Soc. Rev.* , 2012, **41**, 797-828.

7 X. Zhang, L. Y. Ji, S. C. Zhang and W. S. Yang, *J. Power Sources*, 2007, **173**, 1017-1023.

8 S. I. Lee, S. Mitani, C. W. Park, S. H. Yoon, Y. Korai and I. Mochida, *J. Power Sources*, 2005, **139**, 379-383.

9 E. Frackowiak and F. Béguin, *Carbon*, 2001, **39**, 937-950.

10 J. C. Chen, Y. Q. Liu, W. J. Li, C. Wu, L. Q. Xu and H. Yang, *J. Mater. Sci.*, 2015, **50**, 5466-5474.

11 B. Fang, J. H. Kim, M. S. Kim and J. S. Yu, *Acc. Chem. Res.*, 2012, **46**, 1397-1406.

12 L. L. Zhang and X. S. Zhao, Chem. Soc. Rev., 2009, **38**, 2520-2531.

13 E. Raymundo-Pinero, M. Cadek and F. Beguin, Adv. Funct. Mater., 2009, **19**, 1032-1039.

14 F. Beguin, K. Szostak, G. Lota and E. Frackowiak, Adv. Mater., 2005, **17**, 2380-2384; W. Gu, M. Sevilla, A. Magasinski, A. B. Fuertes and G. Yushin, Energy Environ. Sci., 2013, **6**, 2465-2476; A. L. Comte, G. Pognon, T. Brousse and D. Belanger, Electrochemistry, 2013, **81**, 863-866.

15 H. M. Jeong, J. W. Lee, W. H. Shin, Y. J. Choi, H. J. Shin, J. K. Kang and J. W. Choi, Nano Lett., 2011, **11**, 2472-2477.

16 Y. Chen, X. O. Zhang, D. C. Zhang, P. Yu and Y. W. Ma, Carbon, 2011, **49**, 573.

17 P. Serp and J. L. Figueiredo, Carbon materials for catalysis, John Wiley & Sons, Hoboken, NJ, 2009.

18 Y. A. Alhamed, *Eng. Sci.*, 2006, **17**, 75-100.

19 J. C. Chen, Y. Q. Liu, W. J. Li, L. Q. Xu, H. Yang and C. M. Li, *Nanotechnol.*, 2015, **26**, 345401.

20 S. Mitani, S. I. Lee, S. H. Yoon, Y. Korai and I. Mochida, *J. Power Sources*, 2004, **133**, 298-301.

21 H. Benaddi, T. J. Bandosz, J. Jagiello, J. A. Schwarz, J. N. Rouzaud and D. Legras, F. Béguin, *Carbon*, 2000, **38**, 669-674.

22 Y. P. Guo, H. Zhang, N. N. Tao, J. R. Qi, Z. C. Wang and H. D. Xu, *Mater. Chem. Phys.*, 2003, **82**,107-115.

23 Y. P. Guo, J. R. Qi, Y. Q. Jiang, S. F. Yang, Z. C. Wang and H. D. Xu, *Mater. Chem. Phys.*, 2003, **80**, 704-709.

24 K. Kuratani, K. Okuno, T. Iwaki, M. Kato, N. Takeichi, T. Miyuki, T. Awazu, M. Majima and T. Sakai, *J. Power Sources*, 2011, **196**, 10788-10790.

25 Z. H. Hu and E. F. Vansant, *Microporous Mater.*, 1995, **3**, 603-612.

26 Y. K. Lv, L. H. Gan, M. X. Liu, W. Xiong, Z. J. Xu, D. Z. Zhu and D. S. Wright, *J. Power Sources*, 2012, **209**, 152-157.

27 H. Zhu, X. L. Wang, F. Yang and X. R. Yang, *Adv. Mater.*, 2011, **23**, 2745-2748.

28 S. Evers and L. F. Nazar, *Acc. Chem. Res.*, 2013, **46**, 1135-1143.

29 E. N. Lee, H. H. Sunwoo, K. Menninen and J. S. Sim, Poult. Sci., 2002, **81**, 632-641.

30 I. Ron, L. Sepunaru, S. Itzhakov, T. Belenkova, N. Friedman, I. Pecht, M. Sheves and D. Cahen, J. Am. Chem. Soc., 2010, **132**, 4131-4140.

31 T. Yamamoto, Hen eggs: their basic and applied science, CRC Press, Boca Raton, 1997.

32 Z. Ma, T. Kyotani, Z. Liu, O. Teresaki and A. Tomita, *Chem. Mater.*, 2001, **13**, 4413-4415.

33 P. X. Hou, T. Yamazaki, H. Orikasa and T. Kyotani, *Carbon*, 2005, **43**, 2624-2627.

34 K. S. Krishna, G. Vivekanandan, D. Ravinder and M. Eswaramoorthy, *Chem.*

Commun., 2010, **46**, 2989-2991.

35 Y. Lei, N. Luo, X. Yan, Y. Zhao, G. Zhang and Y. Zhang, *Nanoscale*, 2012, **4**, 3438-3443.

36 J. Zhou, N. Xu and Z. L. Wang, *Adv. Mater.*, 2006, **18**, 2432-2435.

Table 1 BET measurements and the specific capacitances of C-Xs and C-2-Ys.

Samples	BET surface area ($m^2 g^{-1}$)	Pore volume ($cm^3 g^{-1}$)	BJH pore size (nm)	Specific capacitance ($F g^{-1}$)
C-1	548	0.312	15.25	---
C-2	811	0.377	15.33	205
C-3	411	0.163	17.22	180
C-4	305	0.144	9.58	95
FC	21	0.01	---	18
C-2-600	137	0.184	11.33	---
C-2-700	608	0.357	15.21	194
C-2-800 (C-2)	811	0.377	15.33	205
C-2-900	424	0.27	17.3	158

Figure caption

Fig. 1 SEM images of (a) C-1, (b) C-2 (C-2-800), (c) C-3, (d) C-4, (e) C-2-600, (f) C-2-700 and (g) C-2-900.

Fig. 2 TEM images of C-2-800.

Fig. 3 Raman spectra of C-Xs and C-2-Ys materials.

Fig. 4 Nitrogen adsorption-desorption isotherms of C-Xs and C-2-Ys, BJH desorption pore-size distribution (inset of a and b)

Fig. 5 The wide-scan XPS spectrum of C-2-800.

Fig. 6 Electrochemical performance of C-Xs and C-2-Ys for supercapacitor tested in 3-electrode cell in 1 M H_2SO_4. (a) CV curves at scan rate of 50 mV s^{-1} for C-Xs. (b) Specific capacitances of C-Xs at various charge-discharge current densities. (c) CV curves at a scan rate of 50 mV s^{-1} for C-2-Ys. (d) Specific capacitances of C-2-Ys at various charge-discharge current densities.

Fig. 7 (a) CV curves of C-2-800 electrode with different scan rates. (b) CD curves of C-2-800 with different current densities.

Fig. 8 Nyquist plots of C-Xs and C-2-Ys at a voltage amplitude of 5 mV.

Fig.9 CV cycling test at a scan rate of 50 mV s^{-1} for C-2-800.

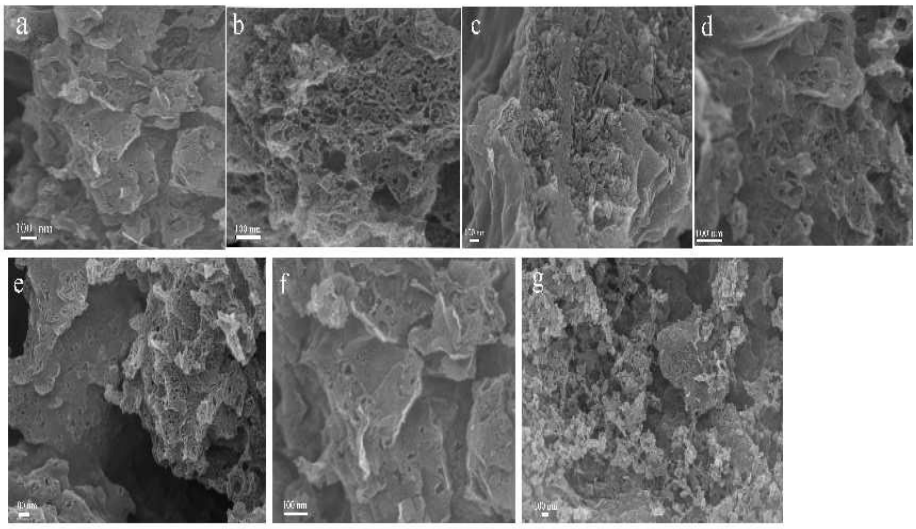

Fig. 1

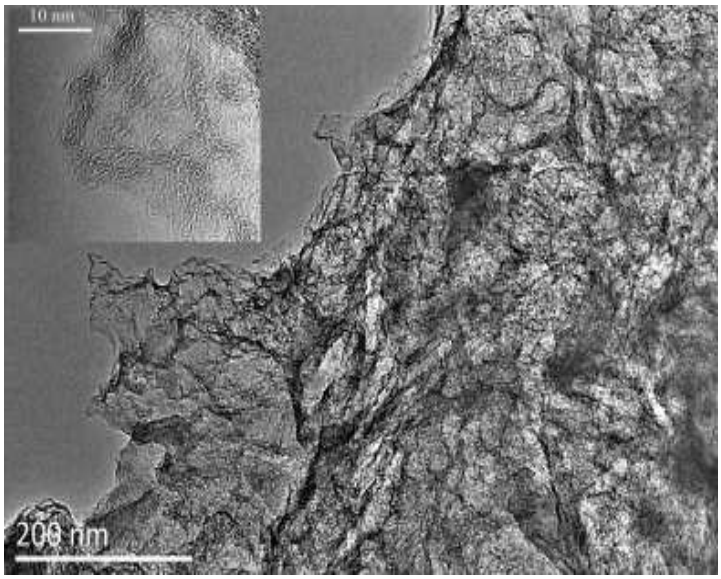

Fig. 2

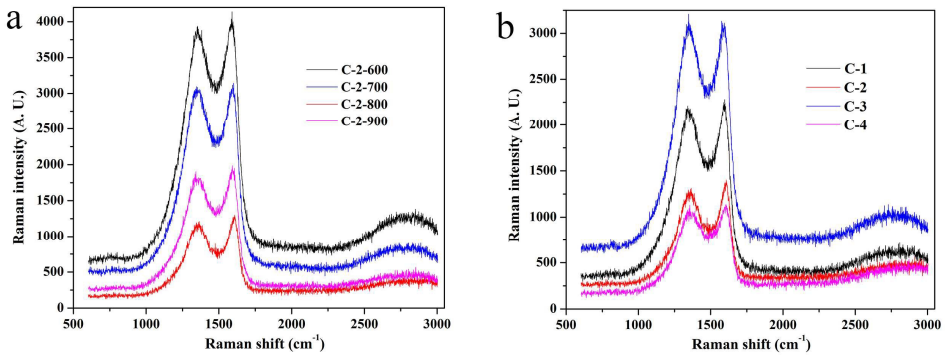

Fig. 3

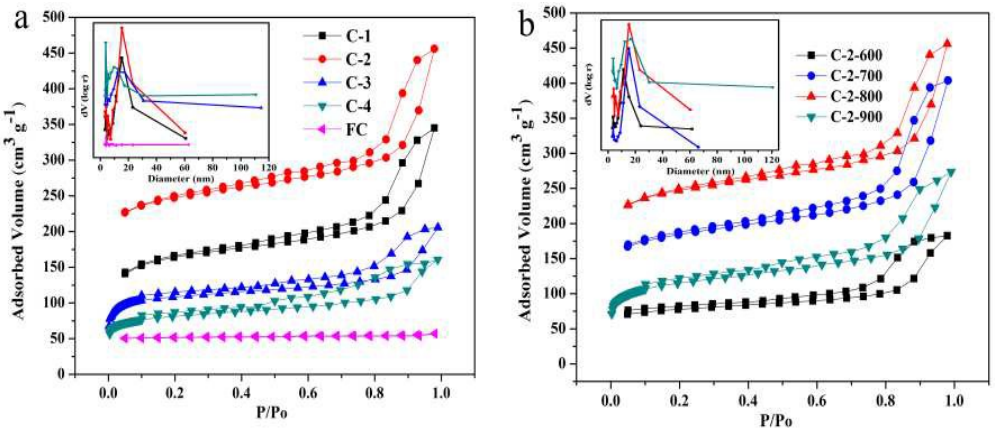

Fig. 4

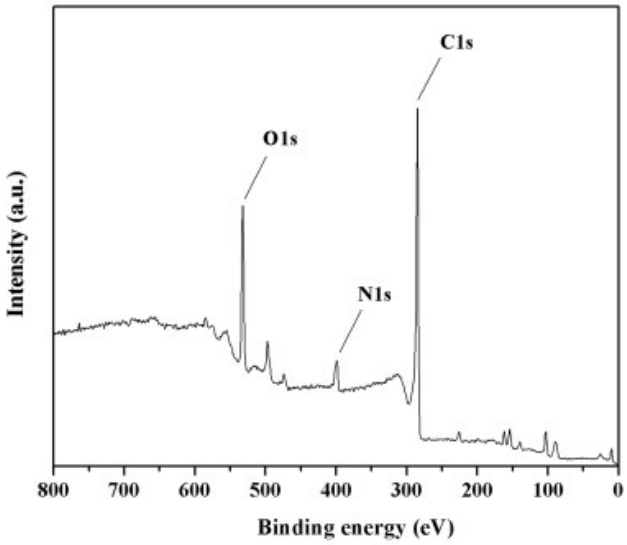

Fig. 5

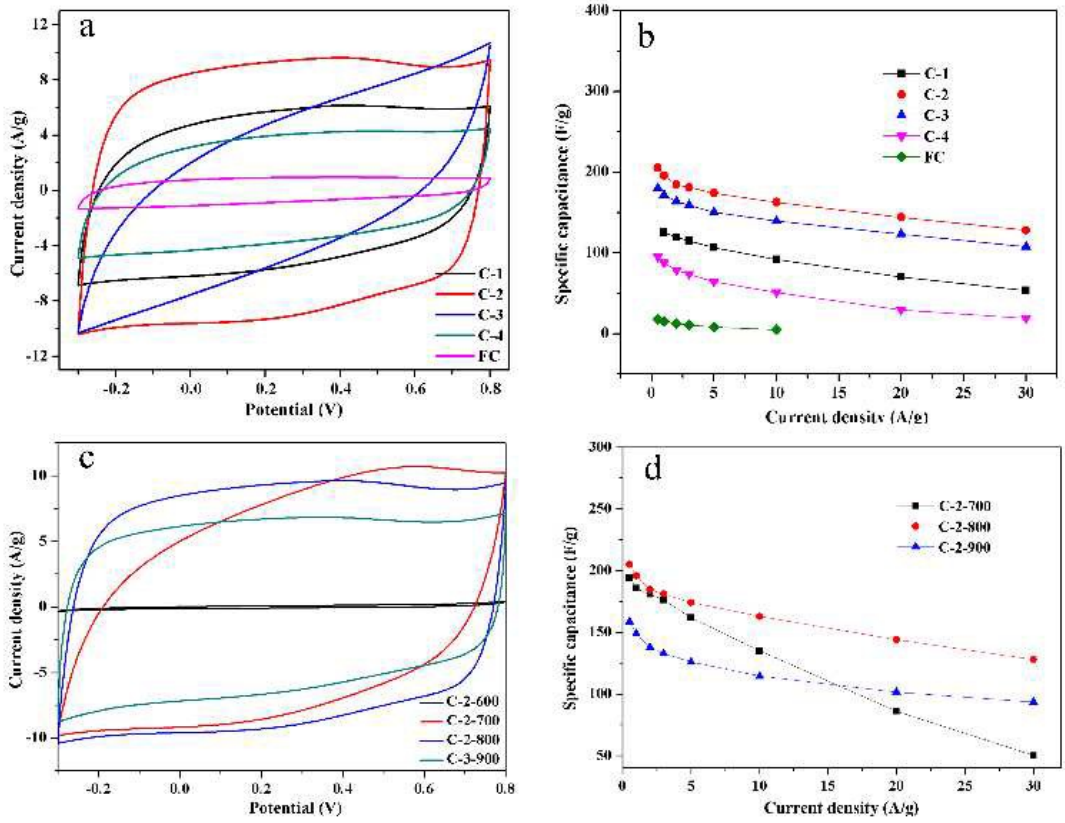

Fig. 6

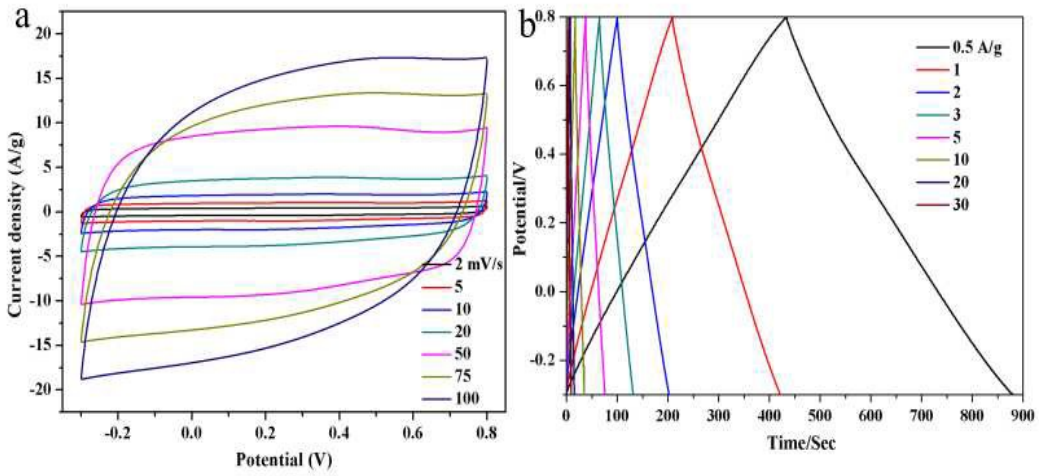

Fig. 7

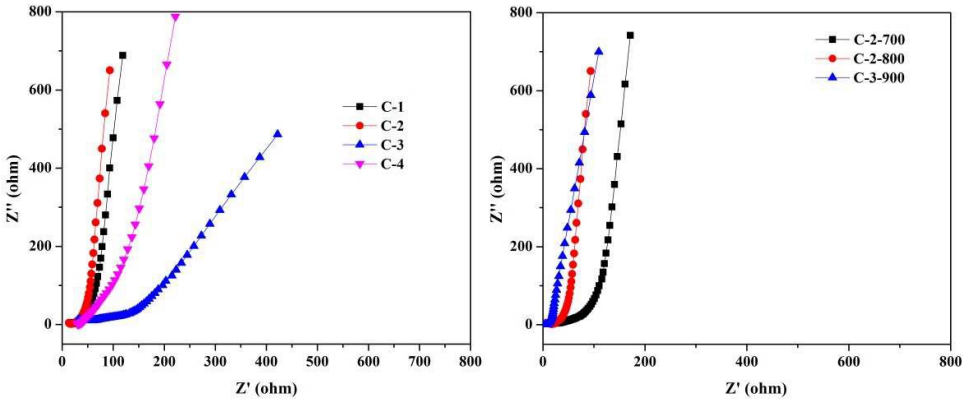

Fig. 8

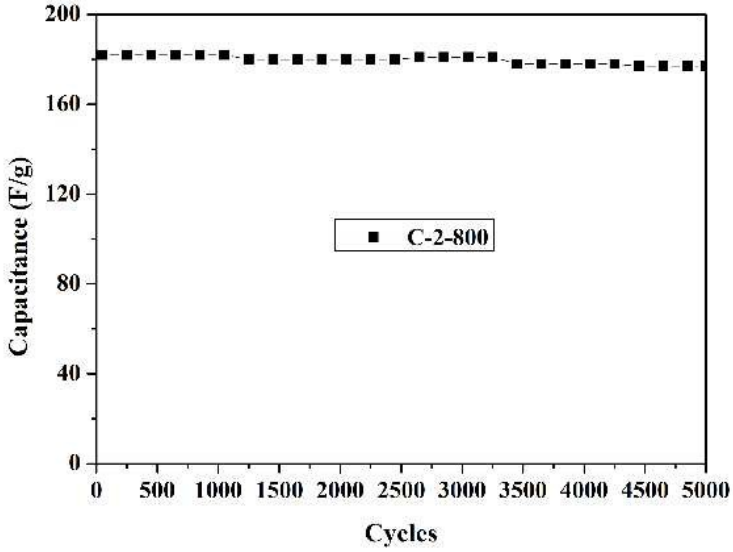

Fig. 9

Title: The large electrochemical capacitance of nitrogen-doped mesoporous carbon derived from egg white by using a ZnO template

Author: Jiucun Chen, Yinqin Liu, Wenjun Li, Huan Yang and Liqun Xu

We used inexpensive and commercially available ZnO nanoparticles as hard template and egg white as precursors to successfully synthesize the nitrogen-doped mesoporous carbon materials and the as-prepared material was further used as an electrode material for supercapacitor applications.